EPJ Web of Conferences will be set by the publisher
DOI: will be set by the publisher
© Owned by the authors, published by EDP Sciences, 2016

PDF and α_s measurements at HERA

Stefan Schmitt[1,a,b]

[1] *DESY, Notkestraße 85, Hamburg, Germany*

Abstract. Recently, the HERA collider experiments H1 and ZEUS combined all available data on inclusive cross section measurements in deep-inelastic scattering (DIS). The resulting Neutral Current (NC) and Charged Current (CC) measurements improve significantly over the individual datasets contribution and also over the previously published combination of a smaller dataset. NC cross sections are measured in the ranges of momentum transfer $0.045 < Q^2 < 50000\,\mathrm{GeV}^2$ and Bjorken-x $0.621 \times 10^{-6} < x < 0.65$ at up to four different centre-of mass energies and, in many points, for both e^+p and e^-p scattering. CC cross sctions are measured in the ranges $300 < Q^2 < 30000\,\mathrm{GeV}^2$ and $0.8 \times 10^{-2} < x < 0.4$ for both e^+p and e^-p. The compatibility of the data with a DGLAP evolution of parton densities is assesed in verious fits. Together with data on jet production in DIS measured at HERA, the strong coupling is extracted at next-to-leading order. New high-precition data on jet production in DIS are compared to next-to-next-to-leading order calculations for the first time.

1 Introduction

At the HERA machine, located at DESY, Hamburg, electrons or positrons of energy 27.6 GeV collided head-on with protons of energies up to 920 GeV. The two experiments H1 and ZEUS collected data in the years 1992-2007, amounting to an integrated luminosity of about $2 \times 0.5\,\mathrm{fb}^{-1}$. Inclusive cross sections, corresponding to the neutral current (NC) reactions $e^\pm p \to e^\pm X$ and the charged current (CC) reactions $e^+p \to \overline{\nu}X$, $e^-p \to \nu X$, have been measured as a function of the momentum transfer Q^2 and the variable Bjorken-x by both collaborations. Here, a combination of all available measurements is presented, together with fits of parton densities and next-to-next-to leading order (NNLO) [1].

In addition to these inclusive cross section measurements, measurements of jet production in the Breit frame in DIS [2–6] are included in fits at next-to-leading order (NLO), to measure the strong coupling $\alpha_s(m_Z)$. New measurements of jet production [7] are also compared to calculations of recently published calculations at NNLO [8].

2 Deep-inelastic scattering

Deep-inelastic scattering of electrons of positrons off a proton proceeds by the exchange of a vector-boson. In the NC process, a photon or Z boson is exchanged, whereas in the CC case a W boson is

[a] e-mail: sschmitt@mail.desy.de
[b] on behalf of the H1 and ZEUS collaborations

exchanged. The kinematics is described by two indepednent variables, for example the momentum transfer $Q^2 = -q^2$, where $q = e - e'$ is the exchanged four-momentum, and the variable Bjorken-x, where $x = Q^2/(2pq)$, with p being the four-vector of the incoming proton. Another variable is the inelasticity $y = 2pq/s$, where s is the centre-of-mass energy squared. The variables are related by the equation $Q^2 = sxy$.

The NC cross section for $e^{\pm}p$ scattering receives contributions from three structure functions, $\tilde{F}_2$, $\tilde{F}_L$ and $x\tilde{F}_3$ and is given by

$$\frac{\mathrm{d}^2\sigma^{\pm}_{NC}}{\mathrm{d}x\mathrm{d}Q^2} = \frac{2\pi\alpha^2}{xQ^4Y_+}\tilde{\sigma}^{\pm}_{NC}, \quad \text{where} \tag{1}$$

$$\tilde{\sigma}^{\pm}_{NC} = \tilde{F}_2 \mp \frac{Y_-}{Y_+}x\tilde{F}_3 - \frac{y^2}{Y_+}\tilde{F}_L. \tag{2}$$

The helicity factors are $Y_{\pm} = 1 \pm (1-y)^2$ and α is the fine structure constant. Higher order electroweak correction have been neglected in the above formulae. The structure function F_2 is dominated by the photon exchange, which is the leading contribution to the cros ssection. By measuring cross sections with e^+ and e^- beams, the structure function $x\tilde{F}_3$ can be measured, which is dominated by the γ-Z

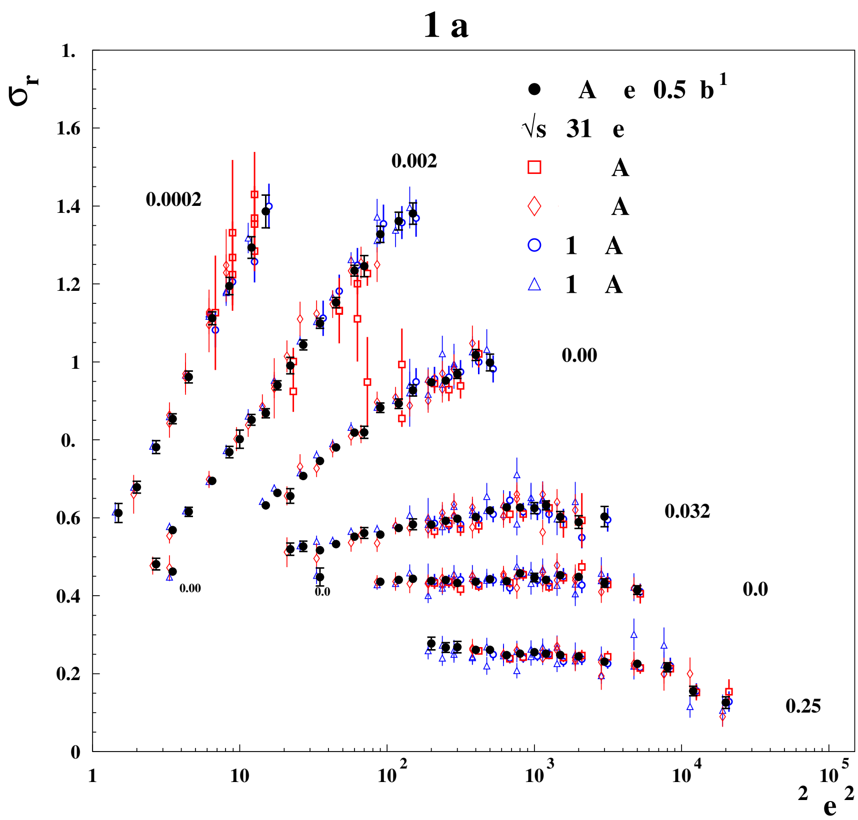

Figure 1. Comparison of selected individual datapoints and the combination results.

interference. The structure function $\tilde{F}_2$ and the longitudinal structure function $\tilde{F}_L$ can be separated by varying y for fixed x and Q^2. For this reason, the HERA machine was operated at different proton beam energies.

The charged current cross section is expressed using structure functions $\tilde{W}_2^{\pm}$, $\tilde{W}_L^{\pm}$ and $x\tilde{W}_3^{\pm}$ by

$$\frac{\mathrm{d}^2\sigma^{\pm}_{CXC}}{\mathrm{d}x\mathrm{d}Q^2} = \frac{G_F^2 M_W^4}{2\pi x}\frac{1}{(Q^2+M_W^2)^2}\frac{1}{2}\left[Y_+\tilde{W}_2 \mp Y_- x\tilde{W}_3^{\pm} - y^2\tilde{W}_L^{\pm}\right]. \tag{3}$$

In the quark-parton-model, the structure functions themselves are related to parton density functions (PDFs) of the proton. The structure functions are all sensitive to different quark flavours, so the HERA data can be used to separate up-type and down-type quark as well as sea and valence quark contributions in PDF fits. Sensitivity to the gluon density originates from the DGLAP equations, which connect PDFs measured at different scales Q^2 and also from the longitidinal structure function.

3 Datasets and data combination

A total of 41 datasets measured by the H1 and ZEUS collaboration are combined. NC cross sections in e^+p scattering are measured at four different proton energies, 460, 575, 820 and 920 GeV, corresponding to four different centre-of-mass energies of 225, 251, 300 and 319 GeV. NC cross sections in e^-p and CC cross sections in e^+p and e^-p are measured at a single centre-of-mass energy, 319 GeV. A total of 2927 data points are combined to obtain 1307 combined cross section measurements. The combination of measurements is illustrated in figure 1. The combined datapoints are much more precise than the individual measurements. Correlated systematic uncertainties are also reduced in the combination procedure [9, 10]. For a given combined datapoint, up to six individual measurements contribute.

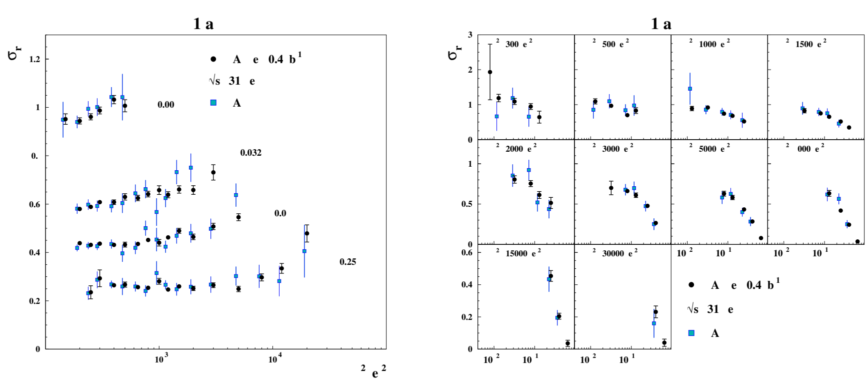

Figure 2. Comparison of the new combined HERA e^-p measurements to the previously published "HERA-I" combination. NC reduced cross sections (left) and CC cross section (right) are shown.

As compared to the previously published combination of a subset of the HERA data, "HERA-I" [11], the improvement is precision is striking, in particular for the e^-p datasets, where the integrated luminosity is increased by a factor of 15. This improvement is shown in figure 2, where the NC and CC cross sections of this combination and the previous combination are compared. The uncertainties are decreased by more than a factor of three in most cases.

4 QCD analsyis of inclusive cross sections

A QCD analysis at NNLO is performed of the combined cros ssection data. The proton PDFs are parameterized at a starting scale $\mu_{f_0} = 1.9\,\mathrm{GeV}$. Using the DGLAP equations [12–16], the PDFs are evolved to arbitrary scales $\mu = Q$, and the predicted DIS cross sections can be compared to theory. The PDF parameters are then determined in a χ^2 minimisation of data and prediction. The HERAPDF2.0 parameterisation used at NNLO has 14 free parameters. Only data with momentum tranfer $Q^2 > Q^2_{\min} = 3.5\,\mathrm{GeV}^2$ are included in the fit. A comparison of the fit results to NC data is

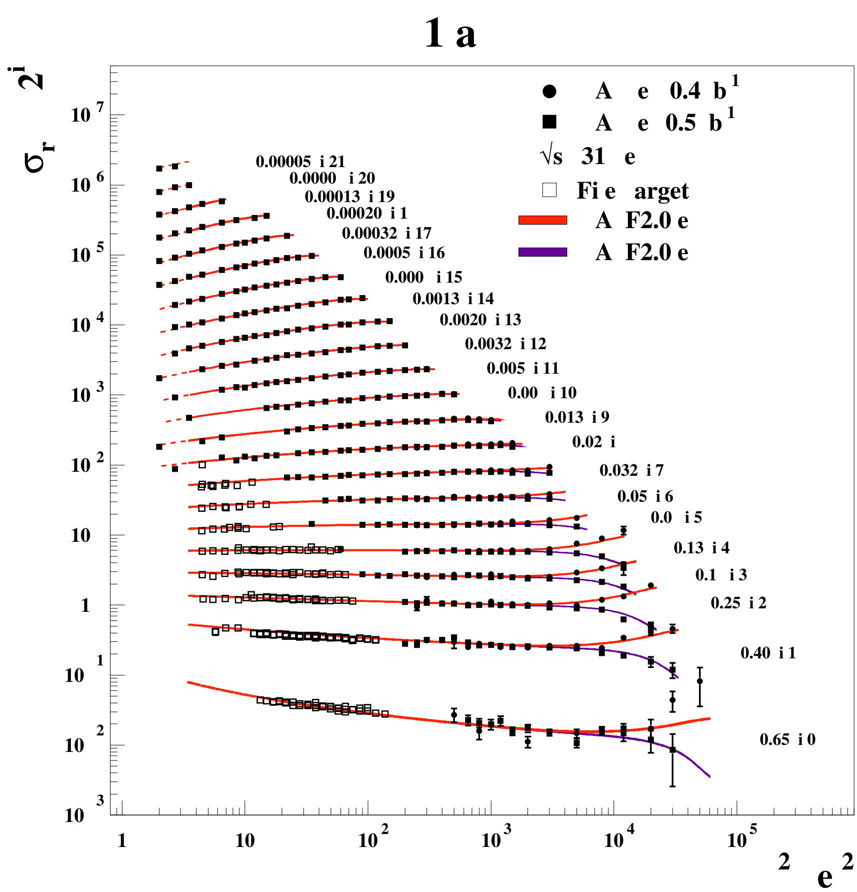

Figure 3. Comparison of the combined HERA NC measurements at $\sqrt{s} = 319\,\mathrm{GeV}$ to the HERAPDF2.0 NNLO fit.

shown in figure 3. The description is very good. At low x, the scaling violations are clearly visible. At high Q^2, the effect of xF_3 is visible, such that the e^-p corss sections are larger that the e^+p cross sections. Overall, the fit yields $\chi^2 = 1363$ for a number of degrees of freedom of 1131. The differences of theory to data are studied as a function of $Q^2_{\min}$, such that data below $Q^2_{\min}$ are excluded from the fit.

The results are shown in figure 4. The fit quality χ^2/d.o.f. improves as $Q^2_{\rm min}$ is increased, but levels out for $Q^2_{\rm min} \gtrsim 10\,{\rm GeV}^2$. IN other words, at lower Q^2 the theory is increasingly less compatible with the data. A detailed comparison of the theory to data at low Q^2 is shown in figure 5; The fit has problems

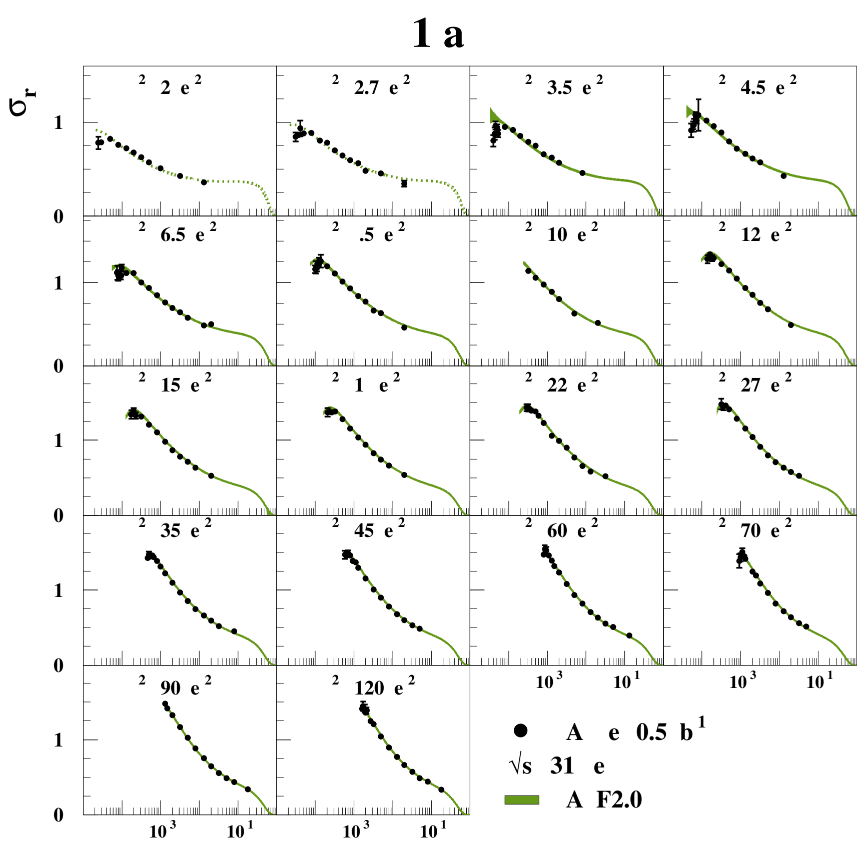

Figure 5. Comparison of the combined HERA NC e^+p measurements at $\sqrt{s} = 319\,{\rm GeV}$ and low Q^2 to the HERAPDF2.0 NNLO fit.

to describe the data at low x and low Q^2, where the longitudinal structure function contributes.

5 Jet data

5.1 Extraction of the strong coupling at NLO

5.2 Comparison to NNLO calculations

6 Summary

References

[1] H. Abramowicz *et al.* [H1 and ZEUS Collaborations], Eur. Phys. J. C **75** (2015) no.12, 580 [arXiv:1506.06042].
[2] S. Chekanov *et al.* [ZEUS Collaboration], Phys. Lett. B **547** (2002) 164 [hep-ex/0208037].
[3] H. Abramowicz *et al.* [ZEUS Collaboration], Eur. Phys. J. C **70** (2010) 965 [arXiv:1010.6167].
[4] F. D. Aaron *et al.* [H1 Collaboration], Eur. Phys. J. C **67** (2010) 1 [arXiv:0911.5678].
[5] A. Aktas *et al.* [H1 Collaboration], Phys. Lett. B **653** (2007) 134 [arXiv:0706.3722].
[6] V. Andreev *et al.* [H1 Collaboration], Eur. Phys. J. C **75** (2015) no.2, 65 [arXiv:1406.4709].
[7] H1 collaboration, "Measurement of Multijet Production in *ep* collisions at Low Q^2 at HERA", H1prelim-16-061 and H1prelim-16-062, publication planned in EPJC.
[8] J. Currie, T. Gehrmann and J. Niehues, Phys. Rev. Lett. **117** (2016) no.4, 042001 [arXiv:1606.03991].
[9] F. D. Aaron *et al.* [H1 Collaboration], Eur. Phys. J. C **63** (2009) 625 doi:10.1140/epjc/s10052-009-1128-6 [arXiv:0904.0929 [hep-ex]].
[10] A. Glazov, AIP Conf. Proc. **792** (2005) 237. doi:10.1063/1.2122026
[11] F. D. Aaron *et al.* [H1 and ZEUS Collaborations], JHEP **1001** (2010) 109 doi:10.1007/JHEP01(2010)109 [arXiv:0911.0884 [hep-ex]].
[12] V. N. Gribov and L. N. Lipatov, Sov. J. Nucl. Phys. **15** (1972) 438.
[13] V. N. Gribov and L. N. Lipatov, Sov. J. Nucl. Phys. **15** (1972) 675.
[14] L. N. Lipatov, Sov. J. Nucl. Phys. **20** (1975) 94.
[15] Y. L. Dokshitzer, Sov. Phys. JETP **46** (1977) 641.
[16] G. Altarelli and G. Parisi, Nucl. Phys. B **126** (1977) 298.

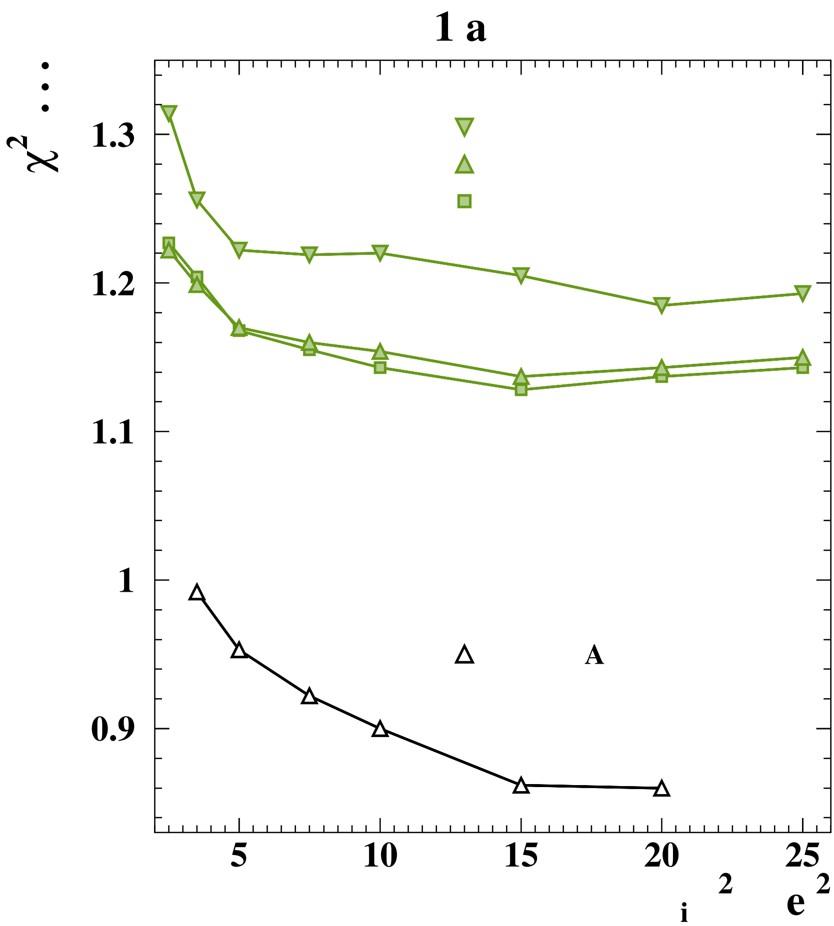

Figure 4. Agreement of data and the fit, χ^2/d.o.f. as a fuinction of $Q^2_{\rm min}$. Data qith $Q^2 < Q^2_{\rm min}$ are excluded from the fit. Fits at LO, NLO and NNO are studied as well as the fit quality for the previously published data combination at NLO.